Preparation of Protein-Resistant Surfaces on Poly(vinylidene fluoride) Membranes via Surface Segregation

J. F. Hester, P. Banerjee, and A. M. Mayes*

Department of Materials Science and Engineering, Massachusetts Institute of Technology, 13-5066, 77 Massachusetts Avenue, Cambridge, Massachusetts 02139

Received May 4, 1998; Revised Manuscript Received December 17, 1998

ABSTRACT: Self-organizing blends of an amphiphilic comb polymer having a poly(methyl methacrylate) (PMMA) backbone and poly(ethylene oxide) (PEO) side chains in poly(vinylidene fluoride) (PVDF) have been examined as a means to create foul-resistant, self-healing surfaces on polymer membranes. X-ray photoelectron spectroscopy (XPS) analysis of phase inversion membranes prepared from these blends indicates substantial surface segregation of the amphiphilic component, which occurs both during the coagulation step of the phase inversion process and in subsequent annealing of the membranes in water. With annealing, a near-surface coverage of nearly 45 vol % comb polymer is produced on a membrane with a bulk comb concentration of only 3 vol %. Surface enrichment of the hydrophilic comb polymer is shown to impart significant resistance to the adsorption of bovine serum albumin (BSA). XPS analysis of membranes treated with concentrated acid shows that hydrophilic surface layers removed by acid exposure may be regenerated by further surface segregation during a subsequent heat treatment in water, resulting in partial recovery of protein adsorption resistance.

Introduction

Filtration of oil- and protein-containing solutions using polymer membranes is strongly limited by fouling of the membrane surface and pores, which results in decreased permeate flux and changing solute selectivity with time. This is a significant economic limitation—membrane cleaning and replacement costs associated with fouling in ultrafiltration (UF) water treatment processes have been estimated to account for 47% of the total process costs.[1] An important cause of fouling is the attraction[2] of organics in the feed water to the typically hydrophobic materials, such as polysulfones, polypropylene, and poly(vinylidene fluoride) (PVDF), which are used in membrane applications due to their excellent chemical resistance and thermal and mechanical properties. Fouling of membranes prepared from hydrophilic materials such as cellulose acetate and polyamides is less severe and often reversible.[3] However, these membranes have comparatively poor mechanical and thermal stability. Moreover, they are susceptible to chemical attack: cellulose acetate membranes are subject to hydrolysis,[4] while polyamide-based membranes are sensitive to oxidants such as chlorine.[5] The ideal membrane would combine the superior bulk properties of the hydrophobic materials with the surface chemistry of the hydrophilic materials.

Several strategies to impart surface hydrophilicity to conventional hydrophobic membrane materials have therefore been investigated. Most methods have focused on the coating or grafting of hydrophilic species onto membrane surfaces. Coating has been accomplished by dipping or spraying steps during membrane fabrication[6,7] or by adsorption of water-soluble polymers or amphiphiles onto completed membranes in aqueous solution.[8,9] Covalent grafting of hydrophilic moieties onto the surfaces of membranes has been achieved by surface graft polymerization of monomers or macromonomers from solution. For this purpose, reactive groups may be produced on membrane surfaces by exposure to low-temperature plasma[10−13] or UV,[14,15] γ-ray,[16] or electron beam[17] radiation.

Each of the above techniques suffers from one or more of the following disadvantages. First, modifying agents confined to the membrane surface are subject to removal during operation or during aggressive cleaning procedures. Coated surface layers are especially easily removed, particularly by changes in solution pH.[6] Second, grafting and coating typically result in changes in the membrane pore size distribution,[6,9,14] often resulting in reduced permeability. Third, these surface modifications impart hydrophilicity to the membrane separation surface only, while foulant accumulation has been observed not only at the separation surface but also within the pore channels of fouled membranes.[8,18,19] Finally, all of the above methods require additional processing steps, which may be quite complex in the case of surface graft polymerization.

An appealing alternative approach might be the utilization of self-organizing blends of hydrophilic and hydrophobic polymers as materials for water treatment membranes with engineered fouling resistance. Here we report preliminary studies on surface enrichment of an amphiphilic comb additive component having a poly(methyl methacrylate) (PMMA) backbone and poly(ethylene oxide) (PEO) side chains in PVDF during the standard phase inversion process for membrane fabrication. We show that this surface segregation imparts significant protein resistance to inherently hydrophobic PVDF-based membranes in blends containing as little as 5 wt % of the comb additive. Moreover, we demonstrate that the hydrophilic surface layers so generated are *self-healing*, in that a foul-resistant layer removed from the surface during operation or cleaning can be substantially regenerated by further segregation of the comb additive upon subsequent heat treatment.

Two processing steps in the standard phase inversion method for membrane fabrication are utilized to achieve the desired surface segregation. The first is the coagula-

* To whom correspondence should be addressed.

10.1021/ma980707u CCC: $18.00
Published on Web 02/18/1999

tion step, during which a thin film of a casting solution composed of polymer dissolved in a solvent is immersed in water, a nonsolvent for the polymer. Water replaces the solvent in the casting solution, until precipitation of polymer occurs at some critical water concentration. The resulting porous structure is characteristically asymmetric, with a dense, 0.1−1 μm surface layer overlaying a highly porous, 100−200 μm sublayer.[20]

The formation of the dense surface layer is brought about by steep gradients in water concentration which exist at early times near the interface between the casting solution and the water bath. The local gradient in the chemical potential of the polymer scales approximately with the local concentration gradient of water,

$$\nabla\mu_{\text{polymer}} \sim \nabla c_{\text{water}} \tag{1}$$

This gradient in polymer chemical potential, in turn, results in a macroscopic flux of polymer directed into the casting solution. The local magnitude of this flux scales with the magnitude of the local gradient in polymer chemical potential,

$$\vec{J}_{\text{polymer}} \sim -\nabla\mu_{\text{polymer}} \tag{2}$$

according to the diffusion equation. It is this flux of polymer into the casting solution prior to precipitation, having a maximum magnitude near the interface, which results in the formation of the dense surface layer of the membrane.[21]

For a polymer blend composed of a hydrophilic component A and a hydrophobic component B, we expect the chemical potential of the hydrophilic component in pure water to be substantially less than that of the hydrophobic component. Thus, we expect that, near the interface,

$$|\nabla\mu_{\text{A}}| < |\nabla\mu_{\text{B}}| \tag{3}$$

and

$$|\vec{J}_{\text{A}}| < |\vec{J}_{\text{B}}| \tag{4}$$

Component A is transported more slowly into the casting solution than B prior to precipitation, resulting in surface enrichment of the hydrophilic polymer. Further surface segregation may be accomplished by heat treatment of the membrane while it is immersed in water, due to the low interfacial energy between the hydrophilic component and water. Such a heat treatment step is commonly performed during the fabrication of commercial membranes in order to refine the pore size distribution.[22]

The amphiphilic polymer used in this study is specifically designed to impart oil and protein resistance to membrane surfaces. PEO is well-known for its extraordinary ability to resist protein adsorption, which is thought to arise from its hydrophilicity, large excluded volume, and unique coordination with surrounding water molecules in aqueous solution.[23−26] Surface-grafted PEO has rendered UF membranes resistant to oil[12] and protein[14−16] fouling. Selection of a comb architecture with PEO side chains as the additive component creates a high yield of surface-localized PEO for each additive molecule near the surface and prevents bulk crystallization of PEO. Moreover, the comb architecture permits compatibilization of the additive and matrix components through the backbone, by exploiting the well-known miscibility of PVDF and PMMA.[27,28] Synthetic control over the length and frequency of the PEO side chains allows for tunable hydrophilicity, water solubility, and glass transition temperature.

Experimental Section

Methyl methacrylate (Aldrich) and polyoxyethylene methacrylate (MW = 475, Polysciences, Inc.) were separately dissolved in tetrahydrofuran and distilled once over calcium hydride and a second time over trioctyl aluminum. The comb additive [P(MMA-*r*-POEM)] was then synthesized as a random copolymer of these monomers using an inert gas anionic technique described elsewhere.[29] GPC analysis indicated that the copolymer had a polystyrene standard molecular weight and polydispersity of $\bar{M}_{\text{w}}$ = 14 400 g/mol and $\bar{M}_{\text{w}}/\bar{M}_{\text{n}}$ = 1.3. The copolymer was 17.3 mol % POEM (^{1}H NMR), so that roughly one out of every five backbone segments had a pendant methoxy-terminated PEO side chain of ∼9 ethylene oxide units. Although the comb polymer used in this study was synthesized anionically, P(MMA-*r*-POEM) can be synthesized using less expensive free-radical routes.[30] PVDF ($\bar{M}_{\text{w}}$ = 534,000 g/mol) was purchased from Aldrich and used as received.

Membranes were prepared by phase inversion from solutions containing 10% (w/v) PVDF in *N*,*N*-dimethylformamide (DMF). P(MMA-*r*-POEM) was added to some of the solutions to make blends having compositions of 2, 5, 10, and 20 wt % additive, corresponding to bulk volume fractions ϕ_{b} of 3.0, 7.5, 14.6, and 27.7%, respectively. The solutions were cast by pipet onto a glass plate previously cleaned with DMF, which was immediately immersed in deionized water (dW, Millipore Milli-Q, 18.2 MΩ cm) at 20 or 90 °C. Membranes were left in water for ∼10 min after separation from the glass plate and then rinsed in a second bath of dW. Some membranes were subsequently annealed at 90 ± 1 °C while immersed in dW. Membranes for morphology and surface composition studies were freeze-dried (Genesis 25LE, Virtis) and held under vacuum at least overnight. Other membranes were stored in dW until use.

To assess the effect of the additive on membrane morphology, unannealed membranes cast at 20 °C and having various blend compositions were examined by field emission scanning electron microscopy (FESEM) using a JEOL 6320 microscope. The membranes were shadowed with carbon prior to FESEM examination, which was performed at an acceleration voltage of 1 kV.

To determine the near-surface compositions of virgin membranes, XPS analysis was performed on membranes having various bulk compositions, casting conditions, and heat treatment histories. XPS was conducted on a Surface Science Instruments SSX-100 spectrometer (Mountain View, CA) using monochromatic Al Kα X-rays ($h\nu$ = 1486.7 eV) with an electron takeoff angle of 45° relative to the sample plane. Survey spectra were run in the binding energy range 0−1000 eV, followed by high-resolution spectra of the C_{1s} region. Peak fitting of the C_{1s} region was conducted with a linearly subtracted background and with each component of the C_{1s} envelope described by a Gaussian−Lorentzian sum function,

$$F(E) = 2A\left[\frac{m\sqrt{\ln 2}}{W\sqrt{\pi}}\exp\left(-4\ln 2\left(\frac{E-E_0}{W}\right)^2\right) + \frac{1-m}{\pi W\left[1+4\left(\frac{E-E_0}{W}\right)^2\right]}\right] \tag{5}$$

where $F(E)$ is the intensity at energy E, A is the peak area, E_0 is the peak center, W is the full-width at half-maximum, and m is the Gaussian−Lorentzian mixing ratio (1 = pure Gaussian, 0 = pure Lorentzian). The mixing ratio m was constrained

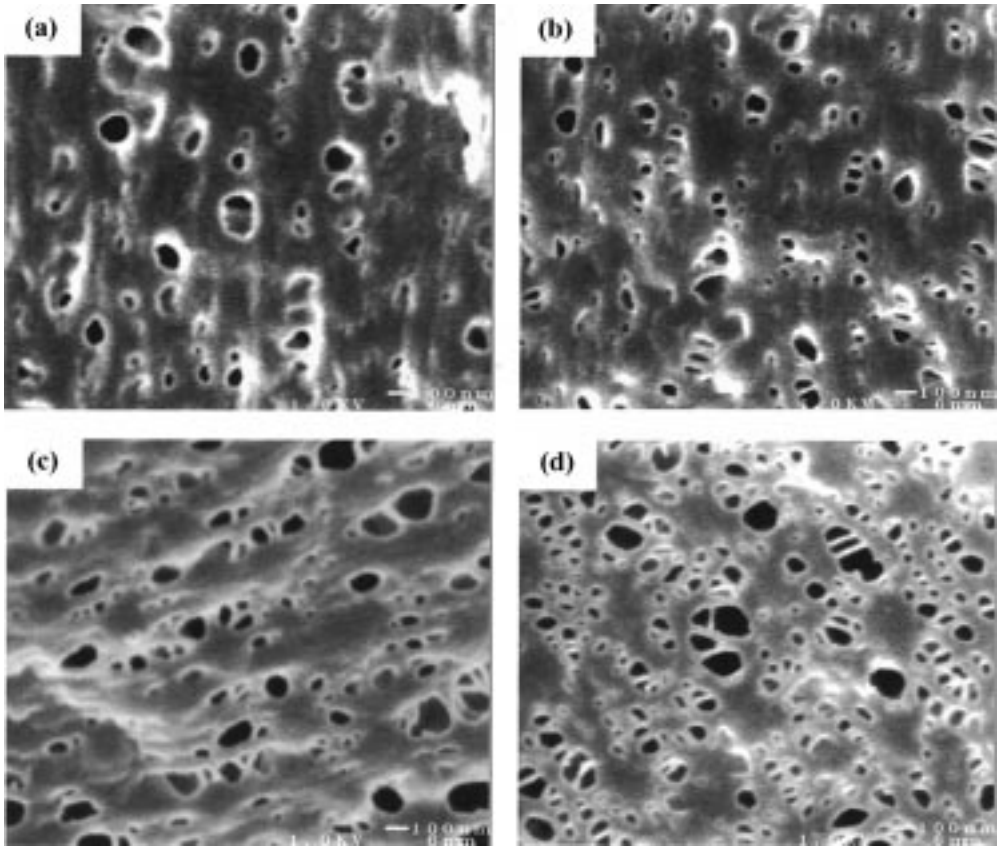

Figure 1. FESEM micrographs of the separation surfaces of unannealed membranes cast at 20 °C, with bulk compositions of (a) 0%, (b) 5%, (c) 10%, and (d) 20% by mass P(MMA-*r*-POEM).

between 0.7 and 1.0 for all fits, a range appropriate to the monochromated Al Kα line shape.[31] Good fits were obtained with peak widths *W* ranging from 1.0 to 1.6 eV.

To investigate protein resistance, unannealed membranes cast at 20 °C and having various bulk compositions were immersed in a solution containing bovine serum albumin (BSA Fraction V, Sigma). Membranes were first washed with phosphate-buffered saline (0.01 M PBS pH 7.4) for 1 h, then incubated in PBS containing 10.0 g/L BSA for 12 h on a rocking table at room temperature, and finally washed in three changes of PBS. Both fouled and virgin membranes were stained for total protein detection using anionic colloidal gold (pH 4, Zymed Laboratories). This technique was developed for the staining of proteins on immunoblots[32] and has been used previously to stain proteins on fouled microfiltration membranes.[11] The anionic colloidal gold particles bind electrostatically to positively charged groups which exist on BSA at pH 4.[33] Fouled and virgin membranes were washed for 5 min with two changes of PBS containing 0.3% (w/v) polyoxyethylene-sorbitan monolaurate (Tween 20, Zymed Labs) as a blocking agent. They were then incubated in PBS + Tween 20 for 1 h at 37 °C and finally washed for 5 min in two changes of PBS + Tween 20 and three changes of dW. The membranes were then incubated in anionic colloidal gold for 4 h on a rocking table at room temperature and rinsed for 5 min in three changes of dW. Finally, the gold-stained membranes were freeze-dried. Surface coverage of the gold label was quantified using XPS. Survey spectra were run in the binding energy range 0−1000 eV, and the near-surface atomic compositions were determined using numerically integrated peak areas and applying standard sensitivity coefficients.

To assess the ability of the hydrophilic surfaces to be regenerated after removal, as-cast (at 20 °C) pure PVDF membranes and as-cast membranes containing 5 wt % P(MMA-*r*-POEM) were immersed for 30 min in chromic sulfuric acid (CSA, KLEAN-AR, VWR). This concentrated acid treatment was intended to simulate the effects of multiple acid cleaning treatments or the long-term presence of oxidants, such as hypochlorite, commonly found in wastewater. The membranes were then heat treated in water for 12 h at 90 ± 1 °C. Samples were cut from these membranes before acid treatment, after acid treatment, and after subsequent heat treatment, and freeze-dried. A control sample of pure P(MMA-*r*-POEM) was spread with a spatula onto a glass slide, exposed to a drop of CSA for 30 min, rinsed with methanol, and dried under vacuum. XPS analysis was conducted on all samples, with peak fitting of the C_{1s} region of the spectra as described above.

To investigate the protein resistance of the regenerated surfaces, as-cast (at 20 °C) membranes containing 5 and 10 wt % P(MMA-*r*-POEM) were exposed to CSA and subsequently heat-treated in water as described above. Samples cut from these membranes before acid treatment, after acid treatment, and after heat treatment were fouled with BSA and stained with anionic colloidal gold as previously described. After freeze-drying, surface coverage of the gold label was again quantified using XPS.

Results and Discussion

Membrane Morphology. Micrographs a−d in Figure 1 are FESEM images obtained at a magnification of 50000× from unannealed membranes cast at 20 °C and containing 2, 5, 10, and 20 wt % comb additive, respectively. For each composition, several randomly selected images were binarized using commercial software (Image-Pro Plus, Media Cybernetics, Silver Spring, MD). The following statistical information was obtained from the binarized images and is summarized in Table 1: mean pore diameter ($\bar{D}$), standard deviation of pore diameter (σ_D), 5-nm bin of pore diameters occurring most frequently (D_{mode}), maximum observed pore diameter (D_{max}), and porosity (ϵ). The porosity is defined as the total area enclosed by pore inlets per unit area of separation surface.

Table 1. Summary of Pore Size Distribution Statistics

ϕ_b (%)	$\bar{D}$ (nm)	σ_D (nm)	D_{mode} (nm)	D_{max} (nm)	ϵ
0.0	45	29	30−35	138	0.036
3.0	42	26	20−25	158	0.020
7.5	37	23	20−25	128	0.038
14.6	48	36	25−30	253	0.078
27.7	40	25	30−35	240	0.092

The morphology of the separation surface appears unaffected by the addition of P(MMA-*r*-POEM) up to a bulk composition of 5 wt %. Membranes containing 10 wt % or more of the hydrophilic additive are characterized by significantly increased porosities, as well as the appearance of a few larger pores. However, the mean and standard deviations of the pore diameters appear insensitive to membrane composition in membranes containing up to 20 wt % additive.

Surface Composition. The C_{1s} regions of the XPS spectra obtained from virgin membranes were fit with seven component peaks representing different chemical environments. The peak centers of the component peaks, referenced to the hydrocarbon peak at 285.0 eV, were constrained (±0.1 eV) as follows: *C*−COO, 285.72 eV; *C*−H (PVDF), 286.44 eV; *C*−O (PEO), 286.45 eV; *C*−O (MMA), 286.79 eV; *C*OO, 289.03 eV; and *C*−F 290.90 eV. These values correspond to values obtained from pure PMMA, PEO, and PVDF homopolymers using high-resolution instrumentation.[31] The areas of the *C*−H and *C*−F peaks of PVDF were constrained to be equal, as required by stoichiometry, as were the *C*−COO, *C*−O, and *C*OO peaks of the methacrylate environment. The ratio of the *C*−O (PEO) and *C*−O (MMA) peak areas was initially constrained to its ideal stoichiometric value of 2.98. Once the peak-fitting routine converged, this constraint was released and fitting was continued in order to allow for the possibility of nonstoichiometric area ratios.

Component peak area percentages from the front sides of the membranes are listed in Table 2. Here, the "front" side refers to the side of the casting solution contacting water when the glass plate is first immersed in the coagulation bath. Near-surface mole fractions of the additive were obtained directly from the ratio of the *C*OO and *C*−F peak areas A_{COO}/A_{C-F}, and these mole fractions were converted to volume fractions using the repeat unit molecular weights and densities given in Table 3.

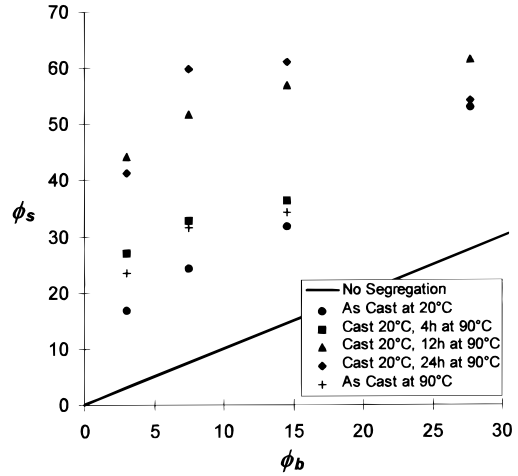

Figure 2. Near-surface concentration of P(MMA-*r*-POEM) versus bulk concentration (vol %) for unannealed membranes cast at 20 and 90 °C and for membranes cast at 20 °C and subsequently heat treated for 4, 12, and 24 h at 90 °C in water.

Figure 2 is a plot of a near-surface concentration of P(MMA-*r*-POEM) versus bulk concentration (both in volume percent) for unannealed membranes cast at 20 and 90 °C, and for membranes cast at 20 °C and subsequently heat-treated for 4, 12, and 24 h at 90 °C in water. The solid line denotes $\phi_s = \phi_b$. Significant surface segregation is observed during the coagulation step of the phase inversion process. The extent of surface segregation in as-cast membranes is increased somewhat by increasing the temperature of the coagulation bath to 90 °C. The surface coverage of the hydrophilic component is substantially enhanced by subsequent heat treatment in water. In fact, an integrated near-surface coverage of nearly 45 vol % is achieved by heat treatment of a membrane with a bulk concentration of only 3 vol %. The actual surface fraction of the additive is likely even higher, since the 45° takeoff angle used in these XPS experiments integrates contributions from a depth of ∼50 Å.[34,35] The fact that the near-surface compositions of annealed membranes appear to reach a limiting value of ∼60 vol % P(MMA-*r*-POEM) suggests that this integrated value might correspond to nearly complete surface coverage of the hydrophilic component. The ratios $A_{C-O(PEO)}/A_{COO}$ for the various membranes had a mean value of 2.77, somewhat less than the stoichiometric value of 2.98. This has been observed

Table 2. C_{1s} Component Peak Areas as Percentages of Total Area for Virgin Membranes, Front Sides

ϕ_b (%)	casting temp (°C)	anneal time (h)	*C*−H	*C*−COO	*C*−H (PVDF)	*C*−O (PEO)	*C*−O (MMA)	*C*OO	*C*−F
3.0	20	0	12.45	1.94	38.16	5.42	1.94	1.94	38.16
3.0	90	0	17.17	2.62	34.02	6.93	2.62	2.62	34.02
3.0	20	4	13.55	3.18	34.00	8.92	3.18	3.18	34.00
3.0	20	12	41.14	3.70	18.58	10.62	3.70	3.70	18.58
3.0	20	24	29.42	4.10	23.09	12.08	4.10	4.10	23.09
7.5	20	0	9.98	2.98	36.83	7.42	2.98	2.98	36.83
7.5	90	0	15.80	3.64	31.25	10.79	3.64	3.64	31.25
7.5	20	4	12.63	3.92	31.97	11.68	3.92	3.92	31.97
7.5	20	12	32.47	5.10	18.96	14.31	5.10	5.10	18.96
7.5	20	24	27.38	6.61	17.61	17.56	6.61	6.61	17.61
14.6	20	0	9.45	3.94	33.65	11.42	3.94	3.94	33.65
14.6	90	0	9.11	4.46	33.96	9.59	4.46	4.46	33.96
14.6	20	4	14.90	4.38	30.51	10.94	4.38	4.38	30.51
14.6	20	12	32.71	5.90	17.81	13.99	5.90	5.90	17.81
14.6	20	24	27.38	6.77	17.11	18.10	6.77	6.77	17.11
27.7	20	0	18.69	6.26	22.01	18.49	6.26	6.26	22.01
27.7	20	12	32.63	6.22	15.49	17.73	6.22	6.22	15.49
27.7	20	24	17.13	6.56	21.94	19.30	6.56	6.56	21.94

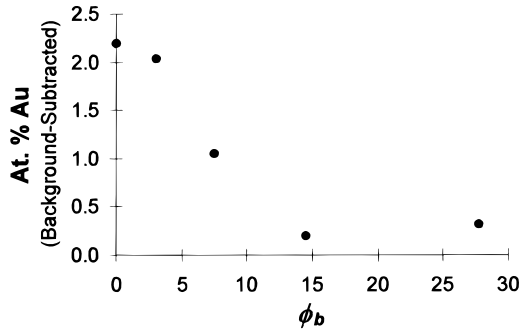

Figure 3. Background-subtracted near-surface gold concentration (atom %) versus bulk concentration P(MMA-*r*-POEM) (vol %) for as-cast (at 20 °C) membranes fouled with BSA and stained for protein detection using anionic colloidal gold.

Table 3. Repeat Unit Molecular Weights and Densities

	M_0 (g/mol)	ρ (g/cm^3)
PMMA	100	1.19
PPOEM	478	1.08
PVDF	64	1.74

previously in XPS analysis of P(MMA-*r*-POEM)[30] and is probably due to preferential orientation of the high-energy PEO side chains away from the dry surface.

The near-surface compositions of the "back" sides of unannealed membranes (data not shown) indicated less surface enrichment of the comb additive compared with the corresponding front sides. This lower level of surface segregation is expected, since, during the coagulation step, gradients in water concentration are less severe at the interface between the casting solution and the glass.[21] XPS data obtained from the back sides of annealed membranes generally showed increased levels of surface enrichment of the additive upon heat treatment, although to a lesser extent than those for the corresponding front sides. This is likely due to the composition profile present in as-cast membranes, which might be expected to feature, near the front side, a decay in the concentration of the hydrophilic component from the surface value to the bulk value over a length scale much larger than the polymer radius of gyration. In contrast, the back side of the membrane is expected to exhibit a more uniform concentration profile on this length scale. In practice, solutes are filtered from the feed solution via the dense separation surface on the front side of the membrane, and the front surface composition is of greater practical interest with respect to fouling resistance.

Protein Adsorption Resistance. After colloidal gold staining, the level of protein fouling of membranes was first assessed visually by the intensity of the red color produced, with deep red indicating heavy fouling and pink indicating less fouling. Some gold-stained virgin membranes appeared a very light pink in color, indicating a low level of nonspecific background staining. XPS analysis was performed on the surfaces of both fouled and virgin gold-labeled membranes to determine the near-surface gold concentration. The near-surface compositions were obtained by integration of the following peaks: Au_{4f} (86 eV), C_{1s} (285 eV), O_{1s} (531 eV), and F_{1s} (685 eV). No other elements were detected in the spectra. Background staining was accounted for by subtracting the gold concentration detected on each virgin membrane from that detected on the corresponding fouled membrane. Figure 3 is a plot of background-subtracted near-surface gold concentration versus bulk concentration of the additive for unannealed membranes cast at 20 °C. Even before heat treatment, significant resistance to BSA adsorption is imparted to the surfaces of membranes due to the presence of the hydrophilic additive component.

Compared to alternative methods for assessing protein adsorption resistance, such as radiocounting of adsorbed radiolabeled protein[36] or spectroscopy of adsorbed and eluted chromophore-labeled protein,[15] the technique used here has the benefit that it probes protein adsorption solely on or near the separation surface and not on the internal pore channels deep within the membrane. This is vital for the purposes of this study, since the internal surface area available for protein adsorption likely varies with membrane composition. The method used here has the disadvantage that, due to the photoelectron mean free path length of ~70 Å,[34] the relative area of the Au_{4f} peak in the XPS spectrum may exhibit a slight dependence on the morphology of the adsorbed protein layer (i.e. thick, discrete "islands" versus a uniform film), as well as the obvious dependence on the mass of adsorbed protein per unit surface area. The protein adsorption data presented in this paper should thus be interpreted as a qualitative indication of protein resistance. Ongoing ultrafiltration studies will more quantitatively evaluate the fouling characteristics of membranes composed of these blends.

Surface Regeneration. XPS spectra obtained before and after acid treatment from pure PVDF membranes, pure P(MMA-*r*-POEM), and membranes containing 5 wt % comb additive are displayed in Figure 4. A spectrum obtained from the 5% membrane after exposure to acid and subsequent heat treatment in water is also shown. The surface chemistry of the pure PVDF membrane was unchanged by immersion in acid. To fit the XPS spectrum for the pure comb polymer after acid treatment, it was necessary to shift the position of the *C*OO peak to 289.41 eV, up approximately 0.4 eV from its position prior to acid treatment. A reaction which is facile in concentrated acid and which would result in such a shift is partial hydrolysis of the methacrylate ester group, followed by attack of the acid group on the carbonyl of its adjacent ester to form the anhydride (Figure 5).[37] The anhydride carbonyl has been assigned a position of 289.4 eV using high-resolution equipment.[31]

In any case, due to the apparent change in the chemistry of the carbonyl after acid exposure, it was not possible to distinguish between the *C*−O (MMA) and *C*−O (PEO) environments using the assumption of equal *C*−O (MMA) and *C*OO component peak areas. Thus, XPS spectra for the regeneration study were fit using a single *C*−O peak with the position constrained at 286.62 ± 0.15 eV. The *C*OO peak position was allowed to shift up to 289.41 eV for acid-treated samples. With these exceptions, fitting of the C_{1s} spectra was conducted as described above for the surface composition study. Component peak area percentages for the pure comb and 5 wt % blend samples are listed in Table 4.

Acid treatment of the pure comb sample resulted in a significant reduction of the relative number of carbon atoms having a *C*−O bonding environment (component peak denoted with an arrow). This is probably due to hydrolysis of the PEO side chains to yield soluble fragments, as well as the change in the carbonyl bonding environment noted above. The peak area ratios A_{COO}/A_{C-F}, A_{C-O}/A_{C-F}, and A_{C-O}/A_{COO} for 5 wt %

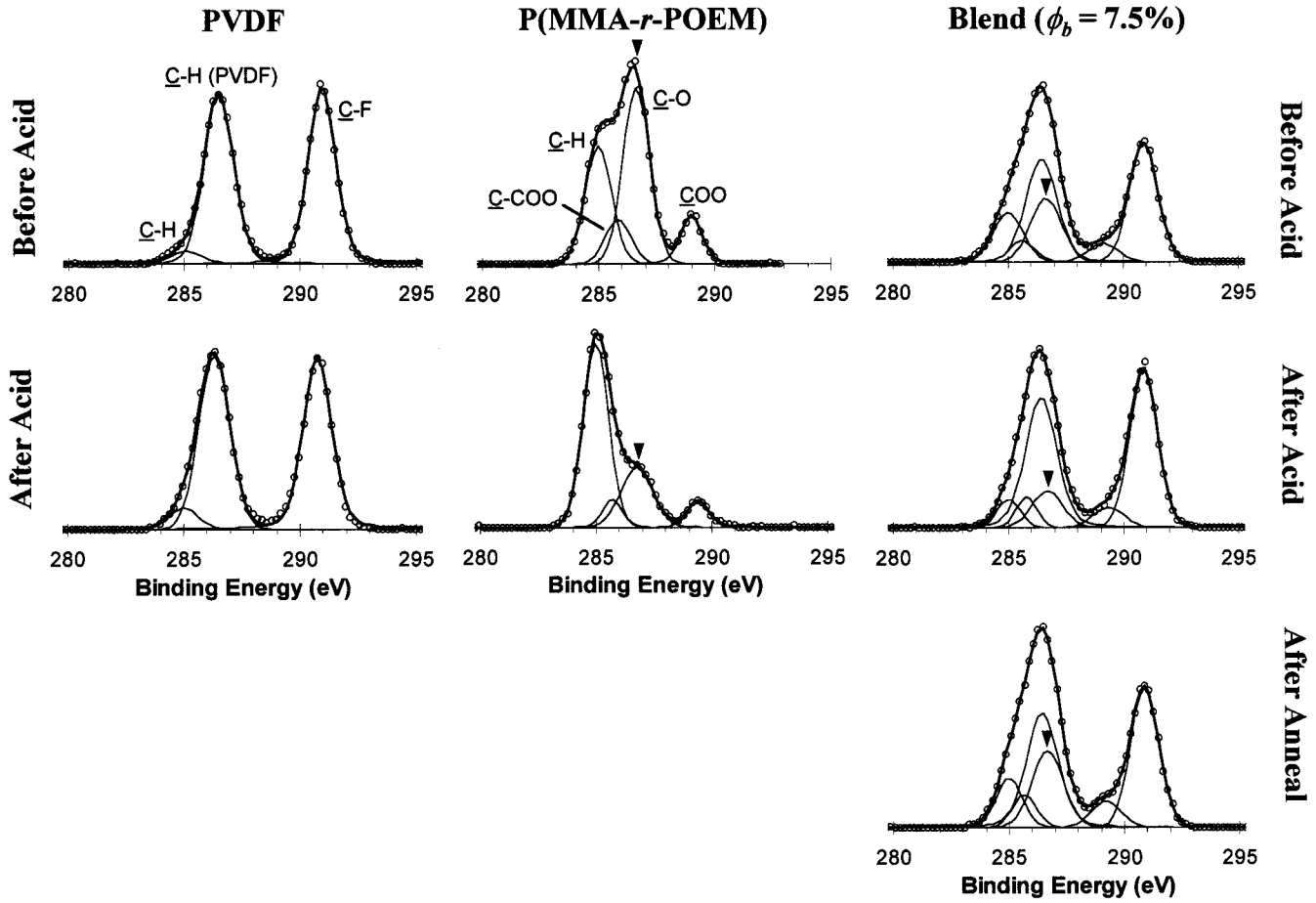

Figure 4. XPS spectra obtained from as-cast and acid-treated PVDF membranes, untreated and acid-treated P(MMA-*r*-POEM), and as-cast, acid-treated, and subsequently annealed membranes containing 7.5 vol % P(MMA-*r*-POEM). All membranes were cast at 20 °C. Arrows denote the component peaks due to the *C*−O bonding environment.

Table 4. C_{1s} Component Peak Areas as Percentages of the Total Area for Samples Used in the Regeneration Study

ϕ_b (%)	history	*C*−H	*C*−COO	*C*−H (PVDF)	*C*−O	*C*OO	*C*−F
100	as cast	31.20	11.32		46.17	11.32	
100	30 min in acid	59.50	7.71		25.08	7.71	
7.5	as cast	12.92	5.06	29.84	17.28	5.06	29.84
7.5	30 min in acid	5.49	5.32	37.22	9.43	5.32	37.22
7.5	30 min in acid + 12 h anneal	9.76	5.95	29.88	18.58	5.95	29.88

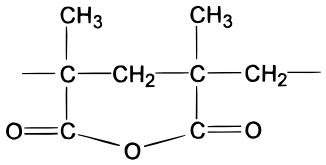

Figure 5. Possible reaction product formed upon exposure of P(MMA-*r*-POEM) to CSA.

Table 5. C_{1s} Component Peak Area Ratios for Blend (ϕ_b = 7.5%) Membranes Used in the Regeneration Study

history	A_{COO}/A_{C-F}	A_{C-O}/A_{C-F}	A_{C-O}/A_{COO}
as cast	0.17	0.58	3.42
30 min in acid	0.14	0.25	1.77
30 min in acid + 12 h anneal	0.20	0.62	3.12

membranes before acid immersion, after acid immersion, and after subsequent heat treatment are listed in Table 5. Acid treatment resulted in a slight reduction in the area of the *C*OO peak relative to that of the *C*−F peak and a substantial reduction in the relative area of the *C*−O peak. This observation is consistent with hydrolysis of the PEO side chains upon immersion in acid, leaving most of the additive backbone intact. Subsequent heat treatment resulted in enhancement of the A_{COO}/A_{C-F} and A_{C-O}/A_{C-F} ratios to slightly greater than their initial, preacid treatment values. These results demonstrate the regenerative capability afforded by the use of a hydrophilic, surface-segregating additive in the membrane composition.

Protein Resistance of Regenerated Surfaces. The near-surface atomic compositions of the stained membranes were determined by integration of the Au_{4f}, C_{1s}, O_{1s}, and F_{1s} peaks in the XPS spectra, as above. Nonspecific background staining was again accounted for by subtraction of the gold concentration detected on each virgin membrane from that detected on the corresponding fouled membrane.

Figure 6 shows the background-subtracted near-surface gold concentrations for membranes containing 5 and 10 wt % P(MMA-*r*-POEM) in the as-cast (at 20 °C) condition, after acid exposure, and after acid exposure and subsequent heat treatment for 12 h in water. The data indicate a dramatic reduction in protein

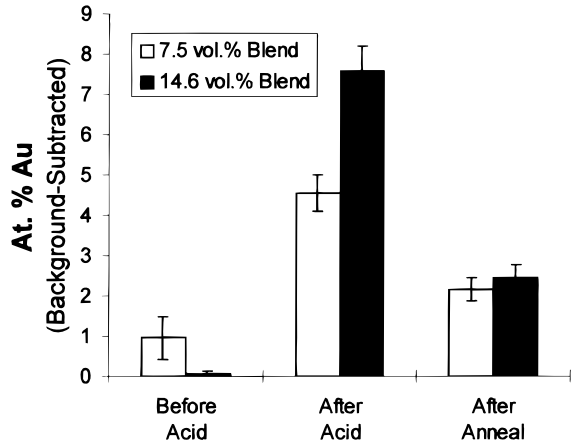

Figure 6. Background-subtracted near-surface gold concentrations (atom %) for as-cast (at 20 °C), acid-treated, and acid-treated and subsequently annealed membranes fouled with BSA and stained for protein detection using anionic colloidal gold.

resistance for both membrane compositions after acid treatment, followed by substantial, though not complete, recovery of protein resistance after heat treatment. It is of interest to note that the membrane with the greater near-surface concentration of P(MMA-*r*-POEM) is significantly *less* protein resistant after acid exposure. This observation indicates that the methacrylate backbone remaining after acid hydrolysis of the comb side chains is more susceptible to protein adsorption than PVDF. This is not surprising, since PVDF, due to its extreme hydrophobicity, has been shown to adsorb BSA less readily than many polymers of intermediate polymer/water interfacial energy, including PMMA.[38] It is likely that, with further annealing, the hydrolyzed comb species would eventually be fully displaced by the more hydrophilic combs from the membrane bulk, providing more complete recovery of protein resistance. Ongoing ultrafiltration studies are aimed at further investigating the recovery of protein and oil resistance in membranes exposed to oxidants.

Conclusions

Significant surface segregation of a comb polymer having a methyl methacrylate backbone and PEO side chains has been shown to occur in PVDF during the coagulation step of the phase inversion process for fabricating polymer membranes. The level of segregation is highest on the separation surface of the membrane, where enrichment of the amphiphilic comb polymer is driven by steep gradients in water concentration near the interface between the casting solution and water at early times during the coagulation step. The level of surface segregation achieved during coagulation is somewhat dependent on the temperature of the coagulation bath, with membranes coagulated at 90 °C showing higher levels of surface enrichment than membranes coagulated at 20 °C.

Further surface localization of the additive component may be accomplished by heat treatment of membranes in water, such that an integrated near-surface coverage of almost 45 vol % is generated on a membrane containing only 2 wt % of the additive in the bulk. PVDF-based membranes containing as little as 5 wt % of the additive display significantly enhanced resistance to BSA adsorption compared to pure PVDF membranes, even before heat treatment. In addition, hydrophilic surface layers removed during a simulated acid cleaning treatment are substantially regenerated by subsequent heat treatment in water, resulting in partial recovery of protein adsorption resistance. Addition of the hydrophilic component has no observable effect on the separation surface morphology of as-cast membranes up to a concentration of 5 wt %, while higher fractions of the comb polymer result in increased porosity and a small proportion of larger pores.

The use of self-organizing blends to generate foul-resistant surface layers on inherently hydrophobic membranes is an appealing alternative to coating and grafting technologies. Surface segregation is accomplished without additional processing steps, reducing the cost of fabrication and the difficulty of scale up. Moreover, the hydrophilic surface layers so produced have a self-healing capacity, due to the small residual concentration of additive in the bulk. Ongoing work is directed toward ultrafiltration of model feed solutions to examine the influence of hydrophilic surface layers so produced on flux decline and separation characteristics.

Acknowledgment. This work was supported in part by the National Science Foundation under Award No. DMR-9357602 and by the MIT Center for Environmental Health Sciences under Public Health Service Grant ESO2109-17. Acknowledgment is made to the donors of the Petroleum Research Fund, administered by the ACS, for partial support of this research. This work made use of MRSEC shared facilities supported by the National Science Foundation under Award No. DMR-9400334.

References and Notes

(1) Gaeta, S. N. In *Membrane Technology: Applications to Industrial Wastewater Treatment*; Caetano, A., de Pinho, M. N., Drioli, E., Muntau, H., Eds.; Kluwer Academic Publishers: Dordrecht, The Netherlands, 1995; pp 25−45.

(2) Koehler, J. A.; Ulbricht, M.; Belfort, G. *Langmuir* **1997**, *13*, 4162−4171.

(3) Aptel, P. In *Membrane Processes in Separation and Purification*; Crespo, J. G., Böddeker, K. W., Eds.; Kluwer Academic Publishers: Dordrecht, The Netherlands, 1992; pp 263−281.

(4) Missimer, T. M. *Water Supply Development for Membrane Water Treatment Facilities*; Lewis Publishers: Boca Raton, FL, 1994; p 31.

(5) Eisenberg, T. N.; Middlebrooks, E. J. *Reverse Osmosis Treatment of Drinking Water*; Butterworth: Stoneham, MA, 1986; p 189.

(6) Nunes, S. P.; Sforça, M. L.; Peinemann, K.-V. *J. Membr. Sci.* **1995**, *106*, 49−56.

(7) Stengaard, F. F. *J. Membr. Sci.* **1988**, *36*, 257−275.

(8) Brink, L. E. S.; Elbers, S. J. G.; Robbertsen, T.; Both, P. *J. Membr. Sci.* **1993**, *76*, 281−291.

(9) Kim, K. J.; Fane, A. G.; Fell, C. J. D. *Desalination* **1988**, *70*, 229−249.

(10) Ito, Y.; Ochiai, Y.; Park, Y. S.; Imanishi, Y. *J. Am. Chem. Soc.* **1997**, *119*, 1619−1623.

(11) Akhtar, S.; Hawes, C.; Dudley, L.; Reed, I.; Stratford, P. *J. Membr. Sci.* **1995**, *107*, 209−218.

(12) Iwata, H.; Ivanchenko, M. I.; Miyaki, Y. *J. Appl. Polym. Sci.* **1994**, *54*, 125−128.

(13) Iwata, H.; Matsuda, T. *J. Membr. Sci.* **1988**, *38*, 185−199.

(14) Thom, V.; Ulbricht, M.; Jonsson, G. *Acta Polytech. Scand., Chem. Technol. Metall. Ser.* **1997**, *247*, 35−50.

(15) Ulbricht, M.; Matuschewski, H.; Oechel, A.; Hicke, H.-G. *J. Membr. Sci.* **1996**, *115*, 31−47.

(16) Mok, S.; Worsfold, D. J.; Fouda, A.; Matsuura, T. *J. Appl. Polym. Sci.* **1994**, *51*, 193−199.
(17) Hautojärvi, J.; Kontturi, K.; Näsman, J. H.; Svarfvar, B. L.; Viinikka, P.; Vuoristo, M. *Ind. Eng. Chem. Res.* **1996**, *35*, 450−457.
(18) Sheldon, J. M.; Reed, I. M.; Hawes, C. R. *J. Membr. Sci.* **1991**, *62*, 87−102.
(19) Kelly, S. T.; Zydney, A. L. *J. Membr. Sci.* **1995**, *107*, 115−127.
(20) Strathmann, H. In *Synthetic Membranes: Science, Engineering and Applications*; Bungay, P. M., Lonsdale, H. K., de Pinho, M. N., Eds.; Kluwer Academic Publishers: Dordrecht, The Netherlands, 1983; pp 1−37.
(21) Strathmann, H.; Kock, K. *Desalination* **1977**, *21*, 241−255.
(22) Chan, K.; Tinghui, L.; Matsuura, T.; Sourirajan, S. *Ind. Eng. Chem. Prod. Res. Dev.* **1984**, *23*, 124−133.
(23) Elbert, D. L.; Hubbell, J. A. *Ann. Rev. Mater. Sci.* **1996**, *26*, 365−394.
(24) Harris, J. M. In *Poly(ethylene glycol) Chemistry: Biotechnical and Biomedical Applications*; Harris, J. M., Ed.; Plenum Press: New York, 1992; Chapter 1.
(25) Lee, J. H.; Lee, H. B.; Andrade, J. D. *Prog. Polym. Sci.* **1995**, *20*, 1043−1079.
(26) Kjellander, R.; Florin, E. *J. Chem. Soc., Faraday Trans. 1* **1981**, *77*, 2053−2077.
(27) Hahn, B. R.; Herrmann-Schönherr, O.; Wendorff, J. H. *Polymer* **1987**, *28*, 201−208.
(28) Ullmann, W.; Wendorff, J. H. *Compos. Sci. Technol.* **1985**, *23*, 97−112.
(29) Walton, D. G.; Soo, P. P.; Mayes, A. M.; Sofia Allgor, S. J.; Fujii, J. T.; Griffith, L. G.; Ankner, J. F.; Kaiser, H.; Johansson, J.; Smith, G. D.; Barker, J. G.; Satija, S. K. *Macromolecules* **1997**, *30*, 6947−6956.
(30) Shard, A. G.; Davies, M. C.; Tendler, S. J. B.; Nicholas, C. V.; Purbrick, M. D.; Watts, J. F. *Macromolecules* **1995**, *28*, 7855−7859.
(31) Beamson, B.; Briggs, D. *High-Resolution XPS of Organic Polymers*; John Wiley & Sons: Chichester, U.K., 1992.
(32) Garfin, D. E.; Bers, G. In *Protein Blotting: Methodology, Research and Diagnostic Applications*; Baldo, B. A., Tovey, E. R., Eds.; Karger: Basel, 1989; Chapter 2.
(33) Moeremans, M.; Daneels, G.; DeMey, J. *Anal. Biochem.* **1985**, *145*, 315−321.
(34) Briggs, D. In *Practical Surface Analysis*; Briggs, D., Seah, M. P., Eds.; John Wiley & Sons: Chichester, U.K., 1983; Chapter 9.
(35) Clark, D. T.; Thomas, H. R. *J. Polym. Sci., Polym. Chem. Ed.* **1977**, *15*, 2843−2867.
(36) Lhoest, J.-B.; Detrait, E.; van den Bosch de Aguilar, P.; Bertrand, P. *J. Biomed. Mater. Res.* **1998**, *41*, 95−103.
(37) Griesser, H. J.; Meijs, G. F. *J. Bioact. Compat. Polym.* **1990**, *5*, 179−193.
(38) Nakamae, K. In *Biomedical Applications of Polymeric Materials*; Tsuruta, T., Hayashi, T., Kataoka, K., Ishihara, K., Kimura, Y., Eds.; CRC Press: Boca Raton, FL, 1993; Chapter 4.3.

MA980707U